AMERICAN SOCIETY FOR MICROBIOLOGY | Journal of Bacteriology®

RESEARCH ARTICLE

DNA Binding and Sensor Specificity of FarR, a Novel TetR Family Regulator Required for Induction of the Fatty Acid Efflux Pump FarE in *Staphylococcus aureus*

Heba Alnaseri,[a] Robert C. Kuiack,[a] Katherine A. Ferguson,[a] James E. T. Schneider,[a] David E. Heinrichs,[a] Martin J. McGavin[a]

[a]University of Western Ontario Department of Microbiology and Immunology, Schulich School of Medicine and Dentistry, London, Ontario, Canada

ABSTRACT Divergent genes in *Staphylococcus aureus* USA300 encode the efflux pump FarE and TetR family regulator FarR, which confer resistance to antimicrobial unsaturated fatty acids. To study their regulation, we constructed USA300 Δ*farER*, which exhibited a 2-fold reduction in MIC of linoleic acid. *farE* expressed from its native promoter on pLI*farE* conferred increased resistance to USA300 but not USA300 Δ*farER*. Complementation of USA300 Δ*farER* with pLI*farR* also had no effect, whereas resistance was restored with pLI*farER* or through ectopic expression of *farE*. In electrophoretic mobility shift assays, FarR bound to three different oligonucleotide probes that each contained a TAGWTTA motif, occurring as (i) a singular motif overlapping the −10 element of the P_{farR} promoter, (ii) in palindrome PAL1 immediately in the 3′ direction of P_{farR}, or (iii) within PAL2 upstream of the predicted P_{farE} promoter. FarR autorepressed its expression through cooperative binding to PAL1 and the adjacent TAGWTTA motif in P_{farR}. Consistent with reports that *S. aureus* does not metabolize fatty acids through acyl coenzyme A (acyl-CoA) intermediates, DNA binding activity of FarR was not affected by linoleoyl-CoA. Conversely, induction of *farE* required fatty acid kinase FakA, which catalyzes the first metabolic step in the incorporation of unsaturated fatty acids into phospholipid. We conclude that FarR is needed to promote the expression of *farE* while strongly autorepressing its own expression, and our data are consistent with a model whereby FarR interacts with a FakA-dependent product of exogenous fatty acid metabolism to ensure that efflux only occurs when the metabolic capacity for incorporation of fatty acid into phospholipid is exceeded.

IMPORTANCE Here, we describe the DNA binding and sensor specificity of FarR, a novel TetR family regulator (TFR) in *Staphylococcus aureus*. Unlike the majority of TFRs that have been characterized, which function to repress a divergently transcribed gene, we find that FarR is needed to promote expression of the divergently transcribed *farE* gene, encoding a resistance-nodulation-division (RND) family efflux pump that is induced in response to antimicrobial unsaturated fatty acids. Induction of *farE* was dependent on the function of the fatty acid kinase FakA, which catalyzes the first metabolic step in the incorporation of exogenous unsaturated fatty acids into phospholipid. This represents a novel example of TFR function.

KEYWORDS *Staphylococcus aureus*, TetR family regulator, antimicrobial agents, efflux pumps, fatty acids

The TetR family of transcriptional regulators (TFR) confers a mechanism of one-component signal transduction employed by bacteria to sense alterations in their environment and convey the appropriate responses (1). To achieve this, sensor and output domains are incorporated into the same polypeptide, as in the prototypic TetR

Citation Alnaseri H, Kuiack RC, Ferguson KA, Schneider JET, Heinrichs DE, McGavin MJ. 2019. DNA binding and sensor specificity of FarR, a novel TetR family regulator required for induction of the fatty acid efflux pump FarE in *Staphylococcus aureus*. J Bacteriol 201:e00602-18. https://doi.org/10.1128/JB.00602-18.

Editor Ann M. Stock, Rutgers University-Robert Wood Johnson Medical School

Address correspondence to Martin J. McGavin, mmcgavin@uwo.ca.

Received 5 October 2018
Accepted 12 November 2018
Accepted manuscript posted online 19 November 2018
Published 11 January 2019

of *Escherichia coli*, which represses the divergently transcribed gene *tetA*, encoding a tetracycline efflux pump. Most TFRs characterized to date conform to this type I arrangement, where the TFR and a divergently transcribed gene that is repressed are separated by an intergenic segment of less than 200 bp (1). In the TetR-TetA paradigm, when tetracycline is present, the antibiotic binds to a C-terminal sensor domain of TetR, promoting a conformational change, such that TetR loses affinity for its operator site, leading to derepression of *tetA* (2). However, there are >200,000 TFR sequences available in protein databases, and among known examples, there is considerable variation, including some that have dual roles as repressor and activator, the ligands that modulate their function, and physiologic processes that are regulated. Thus, while most microbial genomes encode at least one TFR, their functions and mode of regulation are largely undiscovered (1).

In this study, we address the nucleotide binding and sensor specificity of FarR, a novel TFR of *Staphylococcus aureus* that is needed for expression of a divergently transcribed efflux pump, FarE (3). *S. aureus* is a Gram-positive bacterium that asymptomatically colonizes the nose and skin of approximately 30% of humans (4), and yet it is also a major cause of human morbidity and mortality. Consequently, it is exposed to a wide range of environmental conditions encountered at different sites of colonization and infection. Prior to our work, the most detailed knowledge of *S. aureus* TFR function is derived from the plasmid-encoded QacR, a type I TFR that represses a divergently transcribed gene, *qacB,* encoding an efflux pump specific for antimicrobial quaternary amine compounds (5). However, the function and repertoire of chromosomally encoded TFRs in *S. aureus* are less well understood, and just one has been defined in terms of its DNA binding specificity, namely, IcaR, which represses divergently transcribed genes that confer synthesis of an intercellular polysaccharide adhesin (6, 7).

In evaluating how *S. aureus* responds to host-derived unsaturated free fatty acids (uFFA) which are toxic to bacteria (8, 9) and are encountered during colonization and infection (10–12), we isolated fatty acid-resistant (FAR) variants with increased resistance to uFFA, including *S. aureus* FAR7, which harbored a single nucleotide polymorphism that caused an $H^{121}Y$ substitution in a TFR that we named FarR, as a regulator of resistance to antimicrobial fatty acids (3). Like type I TFRs, *farR* is divergently transcribed from the *farE* gene that it regulates, encoding a resistance-nodulation-division (RND) superfamily efflux pump. The expression of *farE* was selectively induced by unsaturated free fatty acids, and *S. aureus* FAR7, which expresses an $H^{121}Y$ variant of FarR, exhibited constitutive *farE* expression, enhanced induced expression, and increased resistance to linoleic acid (3). These observations were consistent with a type I TFR, whereby FarR was expected to repress *farE*, which would be derepressed in response to antimicrobial fatty acids, or through mutations that impair FarR function. However, additional findings did not support this paradigm. Notably, the type I TFR paradigm stipulates that inactivation of a TFR should cause derepression of the divergently transcribed gene, but this was not the case with *farR*, such that *farE* could no longer be induced when *farR* was disrupted by transposon insertion (3).

The sensor specificity of FarR also remains to be determined. Although the sensor domains of some Gram-positive TFRs bind long-chain acyl coenzyme A (acyl-CoA) metabolites, these examples lead to the derepression of genes required for the degradation of exogenous fatty acids (13, 14). However, this metabolic capacity has not been demonstrated in *S. aureus*, where the sole fate of exogenous fatty acid is incorporation into phospholipid through a fatty acid kinase FakA-dependent pathway, and a requirement for acyl-CoA in both fatty acid metabolism and phospholipid synthesis has been excluded (8, 15–17). Therefore, the goal of our present study was to define the role of FarR as a novel TFR in terms of its interaction with target promoters and the specificity of its sensor function.

TABLE 1 MIC of linoleic acid for USA300 and isogenic variants with complementation plasmids

Strain	Plasmid	MIC[a] (μM linoleic acid)
USA300	pLI50	400
	pLI*farE*	>500
USA300 Δ*farER*	pLI50	200
	pLI*farE*	200
	pLI*farR*	200
	pLI*farR7*	200
	pLI*farER*	>500
	pALC2073	200
	pALC*farE*	>400

[a]Data for MIC determinations are presented in Fig. S1.

RESULTS

***farE* cannot confer resistance to antimicrobial fatty acids in the absence of *farR*.** Although we previously noted that *farE* could not be induced in the absence of FarR, this was based on a transposon insertion in the 3′ end of *farR* that would potentially permit the expression of a truncated gene product lacking the C-terminal 37 amino acids (3, 18). Therefore, to precisely define the functions of *farE* and *farR*, we constructed USA300 Δ*farER* and conducted complementation assays with pLI*farE*, pLI*farR*, pLI*farR7*, or pLI*farER,* where the genes are expressed from their native promoters, and pLI*farR7* expresses the variant ^{H121Y}FarR that promotes increased resistance of *S. aureus* FAR7 to linoleic acid (3). USA300 exhibited an MIC of 400 μM, compared to 200 μM for USA300 Δ*farER* (Table 1; see also Fig. S1 in the supplemental material). When complementation plasmids were tested in USA300 Δ*farER*, only pLI*farER* was able to restore resistance, permitting robust growth at 500 μM linoleic acid. Although pLI*farE* did not complement USA300 Δ*farER*, it conferred increased resistance to USA300 (Table 1 and Fig. S1). Since these data supported the contention that *farE* could not be expressed in the absence of *farR*, we queried whether ectopic expression of *farE* would restore resistance, using the $P_{xyl/tet}$ promoter of pALC2073, which permits a basal level of constitutive expression (19). In USA300 Δ*farER*/pALC2073 vehicle, the MIC for linoleic acid was unchanged at 200 μM, compared to >400 μM for USA300 Δ*farER*/pALC*farE* (Table 1 and Fig. S1). From these data, we conclude that FarE-mediated efflux alone is sufficient to promote resistance to linoleic acid, that *farE* cannot be expressed in the absence of *farR*, and that *farR* has no impact on resistance in the absence of *farE*.

Expression of *farR* is autoregulated. Although our data refute the type I TFR paradigm whereby the TFR functions to repress a divergently transcribed gene, another common trait of TFRs is autorepression (1, 20), which we evaluated using a *farR*::*lux* reporter. Although *farR*::*lux* was not strongly expressed at any time during growth of USA300 in tryptic soy broth (TSB), it was strongly derepressed in USA300 Δ*farER* (Fig. 1A). We also compared *farR*::*lux* activity after 3 h of growth in *S. aureus* USA300, USA300 Δ*farER*, and *S. aureus* FAR7 defined by an $H^{121}Y$ substitution in FarR (3). As expected, *farR*::*lux* activity was significantly elevated in FAR7 compared to USA300, and there was another significant increase in USA300 Δ*farER* (Fig. 1B). These data indicate that *farR* is strongly autorepressed by FarR and that ^{H121Y}FarR is a less effective autorepressor.

Identification of promoters and structural features in the *farER* intergenic segment *farER*^{IS}. The divergent *farE* and *farR* genes are separated by a 144-bp intergenic segment (*farER*^{IS}) (Fig. 2A). A Pustell DNA matrix analysis (21) of this segment identified a 17-nucleotide (nt) palindrome, PAL1, with three mismatches, and a 16-nt PAL2, with 4 mismatches (Fig. 2A). PAL1 is comprised of inverted octanucleotide repeats IR1 (5′-AATATACA-3′) and IR2 (5′-TGTAGATT-3′), separated by a single nucleotide. Comparatively, PAL2 on the minus strand has an identical IR1 and variant IR2a with one nucleotide mismatch (5′-TGTAGtTT-3′), but the 5′-to-3′ orientation of these inverted repeats is juxtaposed, represented by 5′-IR2a-IR1-3′. To further define significant sequence motifs, we identified 15 species of coagulase-negative staphylococci

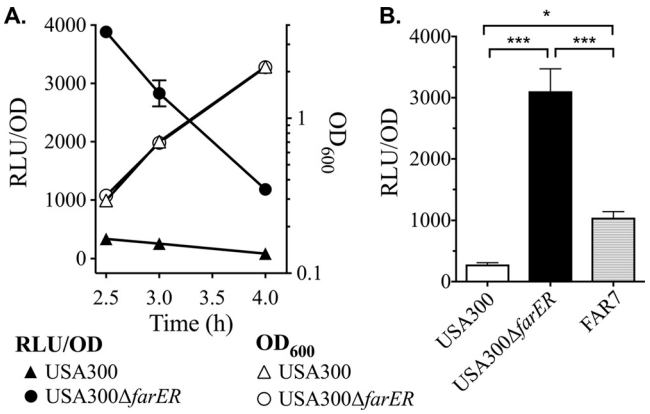

FIG 1 *farR* is regulated by autorepression. (A) Cultures of USA300 or USA300 Δ*farER* harboring pGY*farR*::*lux* were inoculated into triplicate flasks of TSB at OD_{600} of 0.01, followed by incubation at 37°C with orbital shaking. Growth (OD_{600}), and luminescence (relative light units [RLU]) were determined at hourly intervals. Luminescence data were standardized to 1 OD_{600} unit (RLU/OD). All data points represent the mean from triplicate cultures. (B) Luminescence values of *farR*::*lux* (RLU/OD) in cultures of USA300, USA300 Δ*farER*, and FAR7, after growth for 3 h in TSB. Data points represent mean values from triplicate cultures. Statistically significant differences (*, $P < 0.05$; ***, $P < 0.0005$) were determined by Tukey's multiple-comparison test.

with divergent orthologues of *farE* and *farR*, and aligned their intergenic segments to that of *S. aureus* USA300. This revealed three copies of a conserved TAGWTTA motif, two of which overlap the IR2 and IR2a features of PAL1 and PAL2, while a third precedes the IR1 segment of PAL1 (Fig. 2A and S2).

We then resolved to map these features in relation to promoters for *farE* and *farR*. The Berkeley *Drosophila* Genome Project (BDGP) neural network promoter prediction program (22) identified a putative promoter P_{farR} spanning nucleotides 4 to 41 of *farER*^{IS}, and 5′ rapid amplification of cDNA ends (5′-RACE) of RNA extracted from three cultures of *S. aureus* USA300 identified nucleotides at position 3 or 4 within the IR1 segment of PAL1 as +1 transcription start sites (Fig. 2A and S3). A putative P_{farE} promoter was also identified, spanning nucleotides 101 to 63 on the minus strand of *farER*^{IS}. However, several attempts to validate the +1 site by 5′-RACE yielded different nucleotides in the 5′ end of the *farE* coding sequence (data not shown), suggesting that *farE* mRNA is highly sensitive to RNase processing.

FarR and ^{H121Y}FarR exhibit differential binding to oligonucleotide probes spanning *farER*^{IS}. To screen the identified structural features for their interactions with FarR, we conducted electrophoretic mobility shift assays (EMSA) with 6×His-FarR and four overlapping IR-dye-labeled duplex oligonucleotide probes spanning *farER*^{IS} (Fig. 2A and B). Probes OP1, OP2, and OP4 each exhibited a mobility shift in the presence of 6×His-FarR, and each probe has a TAGWTTA motif, either as part of the −10 element of P_{farR} (OP1) or embedded in PAL1 (OP2) or PAL2 (OP4). Conversely, OP3 lacks a TAGWTTA motif and did not interact with 6×His-FarR. Similar results were obtained with ^{H121Y}FarR, except that its interaction with OP1 was strongly attenuated (Fig. 2B). These data are supportive of three binding sites in *farER*^{IS}; two sites associated with PAL1 (OP2) and PAL2 (OP4) are recognized by both native and ^{H121Y}FarR, while a third site in OP1 is strongly bound only by native FarR.

The −10 and +1 features of P_{farR} comprise an operator site for FarR. Since *farR*::*lux* was derepressed in *S. aureus* FAR7, which expresses ^{H121Y}FarR (Fig. 1B), and ^{H121Y}FarR exhibited attenuated interaction with OP1 (Fig. 2B), we reasoned that OP1 has an operator site that facilitates autorepression of P_{farR}. To localize this site, we conducted competition EMSA where IRDye 800-labeled OP1 (^{IRD800}OP1) was mixed with 6×His-FarR and excess nonlabeled overlapping 30mer probes OP1.1, OP1.2, or OP1.3 that span OP1. Of these, only OP1.3 has both the −10 and +1 features of P_{farR}, and was uniquely able to eliminate binding of FarR to ^{IRD800}OP1 (Fig. 2A and C). When

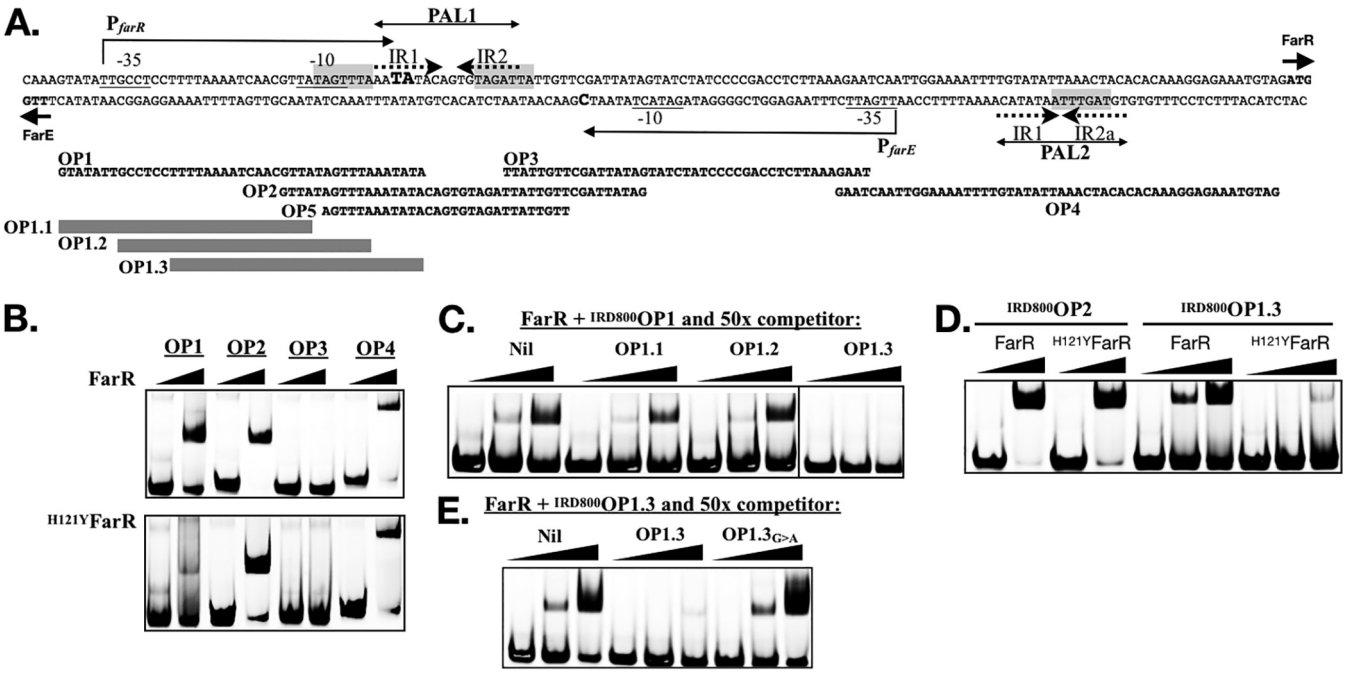

FIG 2 Mapping of structural features in *farER*^{IS} (A) and EMSA to define DNA binding specificity of FarR and ^{H121Y}FarR (B to E). (A) Nucleotide sequence of *farER*^{IS}. The TTG and ATG initiation codons of *farE* and *farR* on the minus and plus strands, respectively, are in bold type and marked with short arrows. Extended arrows above and below the plus and minus strands define the confirmed P_{farR} and predicted P_{farE} promoters, respectively. Nucleotides corresponding to the confirmed P_{farR} +1 transcription start sites are in larger bold type. Nucleotides comprising the −35 and −10 promoter elements of each promoter are underlined. The spans of nucleotides comprising PAL1, PAL2, and the the IR1, IR2, and IR2a inverted repeats are indicated. Shading identifies a TAGWTTA motif that overlaps the −10 element of P_{farR}, as well as the IR2 and IR2a features of PAL1 and PAL2. Nucleotide sequences of overlapping oligonucleotide probes OP1, OP2, OP3, OP4, and OP5 used in EMSA are illustrated below *farER*^{IS}, while gray bars define overlapping probes OP1.1, OP1.2 and OP1.3 that span the OP1 sequence. (B) EMSA with 5 pM of IRDye 800-labeled duplex oligonucleotide probes OP1, OP2, OP3, and OP4, mixed with 0 or 2 μM 6×His-FarR or 6×His-^{H121Y}-FarR. (C) Competition EMSA where 5 pM of IRDye 800-labeled OP1 was mixed with 0, 0.5, or 2 μM 6×His-FarR, without competitor (Nil), or with 50× excess of nonlabeled OP1.1, OP1.2, or OP1.3 duplex probe. The OP1.3 competitor was analyzed on a separate gel with its own Nil control, and the appropriate section of this image was merged with an image of the Nil, OP1.1, and OP1.2 competitors as demarcated by the vertical line that separates OP1.2 and OP1.3. (D) EMSA with 5 pM IRDye 800-labeled OP2 or OP1.3 probe, mixed with 0 or 2 μM 6×His-FarR or 6×His-^{H121Y}FarR, as indicated. (E) Competition EMSA where 5 pM of IRDye 800-labeled OP1.3 was mixed with 0, 0.5, or 2 μM 6×His-FarR, without competitor (Nil), or with 50× excess of unlabeled OP1.3 or OP1.3G→A competitor probe.

EMSA was subsequently conducted with ^{IRD800}OP1.3, FarR promoted a strong mobility shift but ^{H121Y}FarR did not, whereas both proteins interacted equally well with IRDye 800-labeled OP2 (^{IRD800}OP2) (Fig. 2D). To address the significance of the TAGWTTA motif in OP1.3, we synthesized unlabeled duplex probe $OP1.3_{G\rightarrow A}$, where TAGTTTA was altered to TAATTTA, which concomitantly alters the −10 element of P_{farR} from TATAGT, to a consensus TATAAT. When 6×His-FarR and ^{IRD800}OP1.3 were mixed with unlabeled OP1.3 or $OP1.3_{G\rightarrow A}$ in competition EMSA, unlabeled OP1.3 inhibited the mobility shift but $OP1.3_{G\rightarrow A}$ did not (Fig. 2E), indicating that this nucleotide substitution abolished FarR binding. Therefore, the TAGTTTA motif that overlaps the −10 element of P_{farR} constitutes an operator site that we designate $^{-10}P_{farR}$.

FarR preferentially binds to PAL1. Although our EMSA indicate that FarR recognizes $^{-10}P_{farR}$, this site is proximal to PAL1 where another TAGWTTA motif overlaps the IR2 half-site (Fig. 2A). To delineate the interaction of FarR and ^{H121Y}FarR with these sites, we performed EMSA with a panel of 339-bp *farER*^{IS} probes, generated by PCR from pLI*farER* or isogenic variants harboring a G→A substitution in $^{-10}P_{farR}$ (*farER*1^{IS}), substitutions in the IR1 and IR2 features of PAL1 (*farER*2^{IS}), or substitutions in both features (*farER*3^{IS}), as delineated in Fig. 3A. Therefore, each probe is composed of the different 144-bp intergenic segments, flanked by additional nucleotides comprising the 5′ ends of the respective *farE* and *farR* genes.

In EMSA with wild-type *farER*^{IS} and 0.5 μM FarR, two mobility shifts were detected, with approximately equal amounts of the S1 and slower-migrating S2 products (Fig. 3B). With 1.0 μM FarR, S1 was no longer evident and there was only a trace of S2,

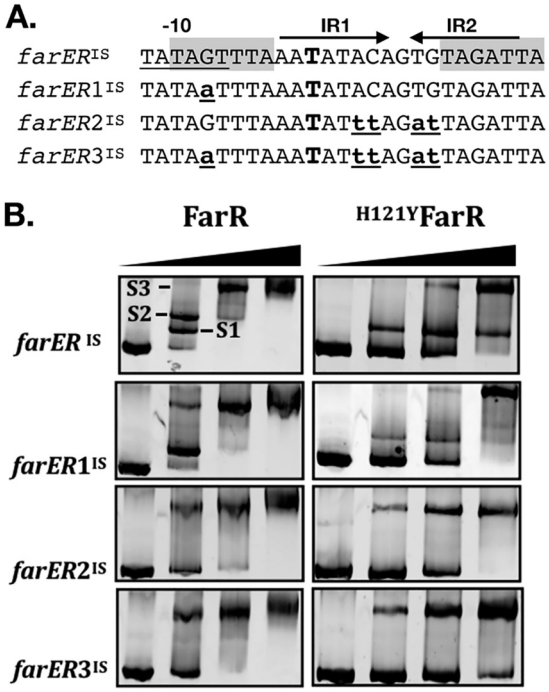

FIG 3 EMSA with 339-bp *farER*^{IS} segment and derivatives to evaluate impact of nucleotide substitutions in FarR operator sites. (A) Nucleotide sequence showing the variable segments of the 339-bp *farER*^{IS}, *farER*1^{IS}, *farER*2^{IS}, and *farER*3^{IS} probes. The labeled features above *farER*^{IS} are as detailed for Fig. 2A. The larger bold type "T" in IR1 indicates the +1 transcription start site of *farR*. Lowercase underlined nucleotides indicate nucleotide substitutions that differentiate each probe. The different EMSA probes were generated by PCR with primer pair *farER*^{IS}-F2 and *farER*^{IS}-R2, using plasmid pLI*farER*, pLI*farER*1, pLI*farER*2, or pLI*farER*3 as the template. (B) EMSA was conducted with 5 pM PCR product and 0, 0.5, 1, or 2 μM FarR or ^{H121Y}FarR, as indicated. The first lane of each panel represents electrophoresis of the *farER*^{IS} probe without added protein (i.e., 0 μM FarR). In the upper-left panel, the protein-DNA complexes S1, S2, and S3 are labeled. Protein-DNA complexes were directly imaged by ethidium bromide staining.

accompanied by appearance of a S3 supershift, which was the only product detected at 2.0 μM FarR. In EMSA with *farER*1^{IS} (G→A substitution in $^{-10}P_{farR}$), the S2 complex was eliminated, indicating that this complex is due to binding of FarR to $^{-10}P_{farR}$. However, both S1 and S2 were eliminated with *farER*2^{IS} in which PAL1 is altered, and a similar result occurred with *farER*3^{IS}, which has substitutions in both $^{-10}P_{farR}$ and PAL1. From these data, it appears that FarR binds preferentially to PAL1, accounting for the S1 complex, followed by binding to the adjacent $^{-10}P_{farR}$ site, accounting for S2. This interpretation was supported by EMSA with ^{H121Y}FarR and wild-type *farER*^{IS}, where S1 was detected but S2 was not (Fig. 3B), consistent with our observation that ^{H121Y}FarR bound poorly to the OP1.3 probe that contains $^{-10}P_{farR}$ (Fig. 2D). Although ^{H121Y}FarR retained the ability to form the S1 complex with *farER*^{IS} probe, the S1 complex was again eliminated in EMSA with *farER*1^{IS} or *farER*2^{IS}, where only the S3 complex was evident.

Significance of the TAGWTTA motif is context dependent. EMSA with the larger 339-bp *farER*^{IS} panel of probes revealed that FarR bound preferentially to PAL1, followed by binding to the adjacent $^{-10}P_{farR}$ (Fig. 3). Since the S3 supershift only appeared after these sites were occupied and was not affected by substitutions in $^{-10}P_{farR}$ or PAL1, we surmised that the S3 complex was due to FarR interaction with PAL2, and that this interaction would be of lesser affinity than that with PAL1. We therefore undertook a more detailed assessment of FarR interaction with PAL1 and PAL2, and the significance of the TAGWTTA motif in these features, relative to that of $^{-10}P_{farR}$, where binding was eliminated through a single G→A substitution.

When EMSA was conducted with 0.5 μM FarR and probe OP5.1, which is composed of PAL1 extended by four nucleotides at each end, a single mobility shift occurred, with

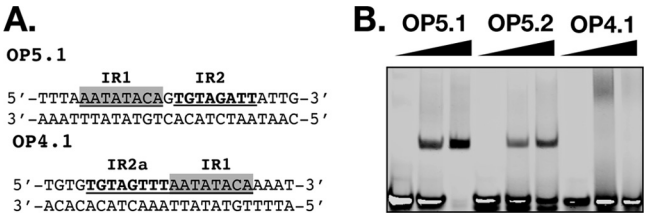

FIG 4 EMSA with minimal PAL1 and PAL2 probes. (A) Composition of PAL1 (OP5.1) and PAL2 (OP4.1) probes. Nucleotides comprising the inverted repeat IR1, IR2, and IR2a components of PAL1 and PAL2 are underlined. The IR1 half-site is shaded, while the IR2 and IR2a half-sites are in bold type. Probe OP5.2 is identical to OP5.1, with the exception of a G→A substitution in the TAGATTA motif that overlaps IR2. The top strand contains a 5′ IRDye 800 addition. (B) EMSA with 0, 0.2, or 0.5 μM FarR mixed with 5 pM OP5.1, OP5.2, or OP4.1, as indicated.

little unbound probe remaining (Fig. 4). With OP5.2 containing a G→A substitution in the TAGWTTA motif of PAL1, complex formation was reduced but not eliminated (Fig. 4B). Therefore, unlike the $^{-10}P_{farR}$ site, where the TAGWTTA motif is a singular feature and the main determinant of specificity, binding of FarR to the higher-affinity PAL1 is more complex. Consistent with our prediction that FarR interaction with PAL2 would be of a lesser affinity, no comparable complex was observed with probe OP4.1 composed of PAL2 extended by four nucleotides at each end (Fig. 4B). Importantly, although PAL1 and PAL2 are composed of similar or identical inverted repeat half-sites, their positions in PAL2 are juxtaposed compared to PAL1 (Fig. 4A).

Nucleotide substitutions in $^{-10}P_{farR}$ and PAL1 alleviate autorepression of *farR* but do not promote increased resistance to linoleic acid. Having established that the interaction of FarR with *farER*^{IS} is altered by nucleotide substitutions in $^{-10}P_{farR}$ and PAL1, we assessed the impact of these substitutions on expression of FarR protein and resistance to linoleic acid. A Western blot of lysates from *E. coli* transformed with native pLI*farR* or pLI*farR*1 harboring a G→A substitution in $^{-10}P_{farR}$ revealed that pLI*farR*1 promoted increased production of FarR protein (Fig. 5A), and reporter gene assays of USA300 transformed with pGY*farR*::*lux* or pGY*farR*1::*lux* confirmed that the G→A substitution in $^{-10}P_{farR}$ caused derepression of P_{farR} (Fig. 5B). We also examined production of FarR protein when *farR* was expressed in the context of pLI*farER* and variants harboring nucleotide substitutions in *farER*^{IS}, as detailed in Fig. 3A. Compared to lysate of *E. coli* plus wild-type pLI*farER*, increased FarR protein was evident in *E. coli*/pLI*farER*1 (Fig. 5A). However, greater FarR production was evident in *E. coli*/pLI*farER*2, consistent with our EMSA data where nucleotide substitutions in PAL1 (*farER*2^{IS}) abrogated FarR binding to both the PAL1 (S1 shift) and $^{-10}P_{farR}$ (S2 shift) sites (Fig. 3B). A similar strong derepression of FarR production was noted with pLI*farER*3 (Fig. 5A), where both the $^{-10}P_{farR}$ and PAL1 are altered. Therefore, nucleotide substitutions within PAL1 abrogate FarR binding to both PAL1 and the adjacent $^{-10}P_{farR}$, leading to strong derepression of *farR* expression.

To evaluate the impact of these substitutions on resistance to linoleic acid, pLI*farER* and derivatives were assessed for their ability to promote growth of USA300 Δ*farER* in TSB plus 50 μM linoleic acid, which normally imparts a 10- to 12-h lag phase on wild-type USA300. Consistent with the ability of pLI*farER* to confer increased resistance, as noted in Table 1, USA300 Δ*farER*/pLI*farER* grew well in TSB plus 50 μM linoleic acid (Fig. 5C). However, growth of USA300 Δ*farER*/pLI*farER*1 was impaired, and USA300 Δ*farER* harboring either pLI50, pLI*farER*2, or pLI*farER*3 failed to enter exponential growth over 8 h of incubation. When grown in TSB alone, all cultures grew equally well (Fig. S4), indicating that increased FarR expression did not affect growth in the absence of fatty acid. Therefore, although *farR* was derepressed as a consequence of nucleotide substitutions in $^{-10}P_{farR}$ or PAL1, this led to diminished resistance.

Sensor specificity of FarR. A tenet of TFR function is that the affinity of a TFR for its operator is modulated by small-molecule ligands (1, 23), including TFRs that bind acyl-CoA (13, 24, 25). Since our EMSA data established that PAL1 harbors the initial site

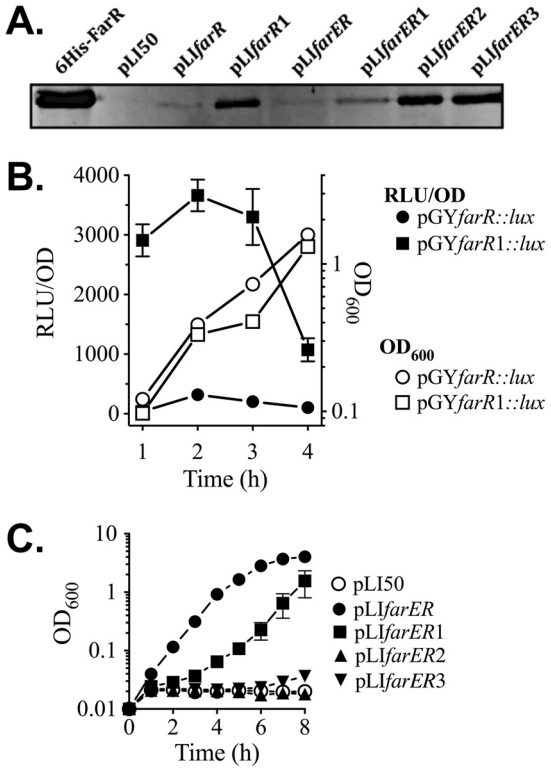

FIG 5 Influence of nucleotide substitutions in $^{-10}P_{farR}$ and PAL1 on expression of FarR, and resistance to linoleic acid. (A) Western blot of gel loaded with 25 ng of purified 6×His-FarR or 25 μg of cell lysate protein from *E. coli* DH5α transformed with pLI50 vehicle, pLI*farR*, or pLI*farER* and derivatives containing nucleotide substitutions in $^{-10}P_{farR}$ (pLI*farR*1 and pLI*farER*1), PAL1 (pLI*farER*2), or $^{-10}P_{farR}$ and PAL1 (pLI*farER*3). (B) Luciferase reporter gene assays of *S. aureus* USA300 transformed with pGY*farR*::*lux*, or pGY*farR*1::*lux* harboring a G→A substitution in $^{-10}P_{farR}$. Triplicates of each culture were grown in TSB, with monitoring of OD_{600} and luciferase activity (relative light units [RLU]) at hourly intervals. Data for RLU determinations are standardized to OD_{600} units (RLU/OD) to account for differences in cell density. (C) Growth of USA300 Δ*farER* complemented with pLI50 vehicle or pLI*farER* and derivatives in TSB plus 50 μM linoleic acid. Each data point represents the mean and standard deviation of the results from triplicate cultures.

of FarR interaction with DNA, we conducted EMSA with 6×HisFarR and probe OP5, composed of PAL1 extended by 6 nucleotides on each end (Fig. 2A), to determine if linoleoyl-CoA or arachidonoyl-CoA could disturb this interaction. However, while linoleic acid and arachidonic acid are both strong inducers of *farE* (3), their acyl-CoA derivatives did not appear to influence the binding of FarR to OP5 (Fig. 6), consistent with a previous report that *S. aureus* does not metabolize exogenous uFFA through acyl-CoA intermediates (15). Rather, the first step in metabolism of exogenous uFFA by *S. aureus* is conversion to an acyl-phosphate through the activity of fatty acid kinase

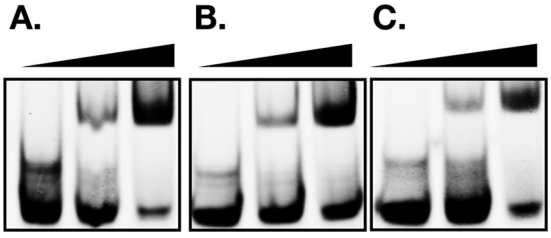

FIG 6 Binding of FarR to OP5 is not diminished by acyl-CoA. EMSA was conducted with 5 pM of IRDye 800-labeled OP5 duplex probe mixed with 0, 0.5, or 2 μM 6×His-FarR only (A) or supplemented with 50 μM linoleoyl-CoA (B) or arachidonoyl-CoA (C).

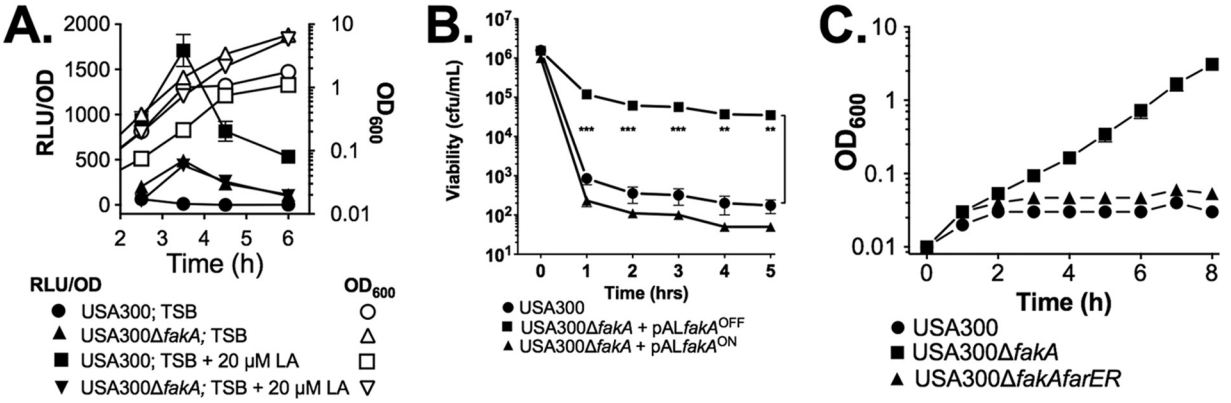

FIG 7 Inactivation of *fakA* causes constitutive expression of *farE* and increased resistance to linoleic acid. (A) Assay of *farE*::*lux* reporter gene in USA300 and USA300 Δ*fakA*. Inoculum cultures were grown overnight in TSB and then inoculated at OD_{600} of 0.01 into TSB only or TSB plus 20 μM LA. Growth (OD_{600}) and luminescence (RLU) were monitored at hourly intervals. Luminescence data were standardized to 1 OD_{600} unit (RLU/OD). All data points represent the mean of the results from triplicate cultures. (B) Assay of viability in TSB containing 100 μM LA. Cultures of USA300 or USA300 Δ*fakA* complemented with pAL*fakA*^{OFF} or pAL*fakA*^{ON} were grown to mid-exponential phase in TSB and then inoculated into TSB plus 100 μM LA at a cell density of 2×10^6 CFU/ml. Cell viability was immediately determined, and after cultures were placed on an orbital shaker, viability was determined at hourly intervals. Each data point represents the mean and standard deviation of the results from triplicate cultures. Asterisks indicate significant differences in viability between USA300 and USA300/pAL*fakA*^{Off} (**, $P < 0.005$; ***, $P < 0.0005$) as determined by multiple *t* test comparisons of viability at each time point using the Holm-Sidak method. (C) Growth assay of USA300, USA300 Δ*fakA*, and USA300 Δ*farERfakA* in TSB plus 50 μM linoleic acid. Inoculum cultures were grown overnight in TSB and then subcultured into TSB plus 50 μM LA at an initial OD_{600} of 0.01. Flasks were incubated at 37°C with orbital shaking, and OD_{600} values were determined at hourly intervals. Each data point represents the mean of the results from triplicate cultures.

FakA (15, 26). To evaluate the contribution of *fakA*, we constructed USA300 Δ*fakA* and compared *farE*::*lux* activity in this background relative to that of USA300.

As previously shown (3), *farE*::*lux* activity was negligible during growth of USA300 in TSB but was induced in TSB plus 20 μM linoleic acid (Fig. 7A). Comparatively, USA300 Δ*fakA* exhibited elevated basal *farE*::*lux* activity during growth in TSB, but expression was no longer responsive to linoleic acid and remained well below the induced level of expression in USA300 (Fig. 7A). Since USA300 Δ*fakA* exhibited elevated noninduced expression of *farE*, we interrogated wild-type USA300 and USA300 Δ*fakA* cells to assess what impact this had on bactericidal activity of linoleic acid (Fig. 7B) and growth in the presence of 50 μM linoleic acid (Fig. 7C). For these experiments, USA300 Δ*fakA* was complemented with pALC*fakA*^{ON} or pALC*fakA*^{OFF}, where *fakA* is cloned in the plus or minus orientation, respectively, relative to the $P_{xyl/tetO}$ promoter in pALC2073. Consequently, USA300 Δ*fakA*/pALC*fakA*^{OFF} retains the *fakA*-null phenotype, while *fakA* expression is restored in USA300 Δ*fakA*/pALC*fak*A^{ON}. Prior to being challenged with a 100 μM bactericidal concentration of linoleic acid, these cultures were grown to exponential phase in TSB, conditions under which *farE* is not expressed in wild-type USA300 but is constitutively expressed in USA300 Δ*fakA*/pALC*fakA*^{OFF}. As expected, USA300 exhibited a rapid loss of viability (Fig. 7B), since expression of *farE* was not induced prior to exposure to 100 μM linoleic acid, whereas significantly greater viability was retained by USA300 Δ*fakA*/pALC*fakA*^{OFF}, consistent with the elevated noninduced expression of *farE*. In contrast, USA300 Δ*fakA*/pALC*fak*A^{ON} behaved as wild-type USA300 (Fig. 7B), suggesting that restoration of *fakA* function eliminated the constitutive expression of *farE*.

To confirm that *farE* was responsible for enhanced resistance, we constructed a USA300 Δ*farERfakA* triple mutant and assessed growth in TSB plus 50 μM linoleic acid. As reported by us previously (3), wild-type USA300 exhibited a 10- to 12-h lag phase (Fig. 7C). However, USA300 Δ*fakA* initiated growth without a lag phase, while USA300 Δ*farERfakA* was unable to grow (Fig. 6C). Therefore, although *farE* cannot be fully induced in USA300 Δ*fakA*, it exhibits sufficient elevated expression to promote increased resistance to linoleic acid.

DISCUSSION

The divergent *farER* arrangement conforms to that of a type I TFR, where in the majority of studied examples, the TFR represses its own expression and the divergently transcribed gene (1), with derepression being achieved in response to a small-molecule ligand that modulates its affinity for operator sites. Our present work describes a variation of this paradigm, with our novel findings including a DNA binding specificity that differs significantly from other *S. aureus* TFRs (5, 6, 27, 28); *farE* cannot be expressed in the absence of FarR function, and induction of *farE* in response to unsaturated fatty acids requires the fatty acid kinase FakA. Since TFRs regulate gene expression in cooperation with a small-molecule ligand and *farE* is only induced in response to unsaturated fatty acids (3), we expected that FarR function would be modified by a fatty acid metabolite as with TFRs that bind fatty acids or acyl-CoA to repress genes required for β-oxidation of fatty acids (13, 25, 29, 30). However, *S. aureus* lacks this metabolic capacity, and exogenous uFFA are metabolized by incorporation into phospholipid (15–17). This is initiated through FakA-dependent phosphorylation, and the acyl-phosphate is used by the PlsY acyl-transferase to acylate glycerol-3-phosphate. Since *S. aureus* does not use acyl-CoA in metabolism of long-chain fatty acids (15, 16), our finding that FakA is required for induction of FarE is consistent with current knowledge on the metabolism of exogenous uFFA in *S. aureus*. However, we cannot conclude that acyl-phosphate is the relevant physiologic ligand.

In addition to acyl-phosphate, FarR function could also be modulated by an unsaturated acyl-acyl carrier protein (acyl-ACP), since exogenous fatty acids that are phosphorylated by FakA can also be used as a substrate by PlsX and converted to an acyl-ACP (26). Accordingly, although TFRs generally bind a small-molecule ligand, a notable exception is DhaS. DhaS is a TFR that regulates dihydroxyacetone kinase expression, but rather than binding dihydroxyacetone, it interacts with the accessory protein DhaQ that forms a complex with dihydroxyacetone (31). Therefore, a number of physiologic ligands are candidates for the modulation of FarR function, which in addition to acyl-phosphate could include acyl-ACP, acyl-glycerol-3-phosphate, or fatty acid kinase in complex with fatty acid.

Although our data demonstrate that FakA is needed to induce *farE* in response to linoleic acid, paradoxically, USA300 Δ*fakA* exhibited an elevated basal level of *farE* expression sufficient to promote increased resistance to linoleic acid. This may be due to the pleiotropic phenotype ascribed to USA300 Δ*fakA*, including an elevated pool of nonesterified fatty acids, leading to reduced transcription of the SaeRS two-component regulator and defective production of Hla toxin (32–34). Broader metabolic changes were also noted, including altered carbon and amino acid metabolism (35). An elevated basal expression of *farE* in response to accumulation of cellular metabolites would be consistent with observations that other RND family efflux pumps also exhibit increased expression in response to an accumulation of cellular metabolites (36–39).

Based on knowledge of TFR function, interaction of FarR with its cognate ligand should modulate its affinity for relevant operator sites, and we identified a TAGWTTA motif as a canonical sequence in all EMSA probes that were bound by FarR. We propose that three occurrences of this motif, each in a distinct context, function to promote respective repression and activation functions. PAL1 contains the primary operator site for autorepression, where the TAGWTTA motif overlaps the IR2 feature (Fig. 2A). Binding of FarR to PAL1 promotes cooperative binding to the adjacent TAGWTTA motif, comprising the $^{-10}P_{farR}$ operator site, and nucleotide substitutions in PAL1 abrogate FarR binding to both PAL1 and $^{-10}P_{farR}$, leading to strong derepression of *farR* expression (Fig. 3 and 5). These findings are compliant with current knowledge of type I TFR function, where the TFR serves to autorepress its expression.

Cooperative binding of FarR to this primary repressor site that regulates *farR* expression resembles that described for AlkX repression of AlkW, a gene required for alkane metabolism in Gram-positive *Dietzia* spp. (30). In this example, AlkX bound to a long 48-bp inverted repeat, causing two distinct mobility shifts, where binding of an

AlkX dimer to a preferred operator half-site facilitated recruitment of a second AlkX dimer to an adjacent site. A different mode of cooperative binding was described for QacR of *S. aureus*, a TFR that represses expression of the QacA efflux pump. In this example, QacR binds to a 28-bp operator as a dimer of dimers, and only one mobility shift was evident irrespective of the amount of QacR used in EMSA (27, 40). For AlkW, it was proposed that this cooperative mode allows for functional repression at lower protein concentrations, so as to better facilitate bacterial adaptation in harsh environments (30).

While our data provide a mechanistic basis for autorepression of P_{farR} by FarR, we have yet to define the means by which FarR promotes *farE* expression. Since *farE* cannot be expressed in the absence of *farR* and cannot be induced in the absence of *fakA*, our model predicts that FarR should promote expression of *farE* in response to a FakA-dependent metabolite of exogenous unsaturated fatty acid, by binding to PAL2, which is upstream of the predicted P_{farE} promoter (Fig. 2A). Since our EMSA was conducted in the absence of exogenous ligand, our initial finding that FarR bound equally well to larger probes containing PAL1 or PAL2 (Fig. 2B) appeared to be inconsistent with such an expectation. However, additional EMSA revealed that FarR retained the ability to bind a minimal PAL1 probe (OP5.1) but not PAL2 (OP4.1) (Fig. 4B), consistent with an expectation that a small-molecule ligand would be required to facilitate specific binding of FarR to the minimal PAL2 site. Such an example was noted with FabR, a TFR that regulates *fabB* required for synthesis and metabolism of unsaturated fatty acids in *E. coli* (41). Notably, binding of FabR to a minimal canonical motif required oleoyl-CoA ligand, but binding also occurred independently of ligand when this minimal motif was extended by additional nucleotides.

Our data have revealed that FarR binds to three different locations within $farER^{IS}$, each harboring a TAGWTTA motif presented in a different context, either as a singular feature in $^{-10}P_{farR}$ or overlapping the IR2 or IR2a half-sites of PAL1 and PAL2. Further adding to the complexity, although PAL1 and PAL2 are composed of identical (IR1) or similar (IR2/IR2a) inverted repeat half-sites, the order of these repeats is juxtaposed in PAL2 relative to PAL1. Although there are few mechanistic examples to compare with other TFRs that activate gene expression, two instances reflect our present findings, whereby the TFR recognizes a canonical motif that occurs in different contexts. SczA is a streptococcal TFR which in the absence of zinc represses a divergently transcribed efflux pump, SczD, by binding a TGTTCA motif that is part of an inverted repeat; however, in the presence of zinc, it activates SczD by binding to an upstream TGTTCA motif embedded in an imperfect palindrome (42). Similarly, LuxR/HapR in *Vibrio* spp. may either repress or activate gene expression through recognition of a TATTGATA motif that can have multiple occurrences in target promoters (43, 44). This motif resembles the IR2/IR2a half-site TGTAGWTT in PAL1 and PAL2 and the $^{-10}P_{farR}$ site TATAGTTT. Therefore, the ability to recognize a common motif in a context-dependent manner may be a general trait of TFRs that function as both repressor and activator.

Based on our present data, combined with consideration of these examples and knowledge of *S. aureus* fatty acid metabolism and its environmental niche, we propose that expression of *farE* is tightly regulated so as to permit expression only when the availability of unsaturated fatty acid exceeds the metabolic capacity for incorporation into phospholipid. Although uFFA are toxic to *S. aureus* if allowed to accumulate in the membrane as free fatty acids, their FakA-dependent esterification into phospholipid represents a means of detoxification (8), which concurrently allows *S. aureus* to optimize its resources by utilizing host-derived fatty acids for phospholipid synthesis. However, sustained efflux of uFFA would be wasteful of resources, such that *farE* may only be expressed when there is an appropriate balance of FarR and its cognate ligand. This may account for our finding that strong derepression of *farR* through nucleotide substitutions in PAL1 is detrimental to resistance, presumably because the physiologic ligand is limiting, and the majority of FarR would be in a ligand-free form. Our future work will focus on resolving these

mechanistic considerations, including a detailed analysis of how FarR interacts with the PAL2 site in the presence or absence of ligand.

MATERIALS AND METHODS

Bacterial strains and growth conditions. Bacteria and plasmids that were used or constructed in this study are listed in Table S1 in the supplemental material. *S. aureus* cultures were maintained as frozen stocks (−80°C) in 20% glycerol and streaked on TSB agar when required. TSB was supplemented, when needed, with 10 μg/ml erythromycin or chloramphenicol for propagation of strains bearing resistance markers. *E. coli* strains were grown on LB agar or LB broth supplemented with 100 μg/ml ampicillin when needed. Unless otherwise stated, all cultures were grown at 37°C, and liquid cultures were incubated on an orbital shaking platform at 180 rpm. When required for growth analyses, inoculum cultures of *S. aureus* were prepared by transferring cells from a single colony into 13-ml polypropylene tubes containing 3 ml of TSB supplemented with antibiotic, as required, followed by overnight incubation. After determination of optical density at 600 nm (OD_{600}), aliquots were subcultured into 25 ml of TSB in 125-ml flasks to achieve an initial OD_{600} of 0.01. To supplement media with fatty acids, a 5 mM stock concentration was first prepared in TSB containing 0.1% dimethyl sulfoxide (DMSO) and then diluted into TSB plus 0.1% DMSO to achieve the desired concentration of fatty acids.

Strain and plasmid construction. Genetic manipulation of *S. aureus* was conducted following established guidelines (45) and as described in our previous work (46–48). All recombinant plasmids were constructed as shuttle vectors in *E. coli* DH5α. The integrity of plasmids isolated from *E. coli* was confirmed by nucleotide sequencing of the cloned DNA fragments, prior to electroporation into *S. aureus* USA300 or isogenic derivatives, using *S. aureus* RN4220 as an intermediate host. Primers used for PCR amplification of gene segments required for plasmid construction are listed in Table S2, based on the reference genome of USA300 FPR3757 (49).

USA300 Δ*farER* containing an in-frame markerless deletion of *farE* (SAUSA300_2489) and *farR* (SAUSA300_2490) was generated using pKOR1 (50). Briefly, ~1-kbp segments that flank *farER* were amplified by PCR with primers *farE*-UP-*attB1* and *farE*-UP-SacII for the upstream segment and *farR*-DW-SacII and *farR*-DW-*attB2* for the downstream segment. The PCR products were digested with SacII, ligated, and incorporated into pKOR1 by treatment with BP Clonase II (Invitrogen), generating $pKOR^{farER}$. USA300 $pKOR^{farER}$ was then subjected to a two-step temperature shift and antisense counterselection, as previously described (50), generating USA300 Δ*farER*. A similar strategy was used to construct USA300 Δ*fakA*, containing an in-frame deletion of the fatty acid kinase gene *fakA*, which has also been named *dak2* or *vfrB* (16, 32, 51).

Plasmids pLI50 and pALC2073 were used for gene complementation (52, 53). Previously described pLI*farR* and pLI*farE* were used to generate pLI*farER*. This was achieved by digesting pLI*farE* with KpnI and SacII to excise a 2.5-kb fragment containing all but the 5′ end of *farE*. This fragment was ligated to pLI*farR* that was digested with the same enzymes to generate pLI*farER*. To construct pLI*farR*1, which harbors a G→A substitution in the −10 promoter element of P_{farR}, pLI*farR* was used as the template in a PCR with Phusion polymerase and complementary plus and minus strand mutagenic primers *farR*1-P and *farR*1-M, following protocols described in the QuikChange site-directed mutagenesis manual (Stratagene). pLI*farR*1 was further modified by digestion with KpnI and SacII, followed by ligation to a 2.5-kb *farE* fragment from pLI*farE* to generate pLI*farER*1. Similar techniques were employed to construct pLI*farR*2 (mutagenic primers *farR*2-P and *farR*2-M) and pLI*farER*2 with nucleotide substitutions in the PAL1 feature. pLI*farR*3 with nucleotide substitutions in both the P_{farR} and PAL1 features was constructed using pLI*farR*1 as the template with mutagenic primers *farR*3-P and *farR*3-M.

To construct the pALC*fakA,* where *fakA* is expressed from the $P_{xyl/tetO}$ promoter of pALC2073, the promoterless *fakA* gene was amplified by PCR with primers *fakA*-pALC-F and *fakA*-pALC-R, digested with KpnI, and ligated into KpnI-digested pALC2073. Similarly, pALC*farE* was constructed by amplifying the promoterless *farE* gene with primers *farE*-pALC-F and *farE*-pALC-R, digestion of the product with SacI, and ligation into SacI-digested pALC2073. The pGY*lux* reporter gene vector (54) was used as described previously (3) to construct a pGY*farR*::*lux* promoter fusion. Briefly, a 248-bp segment spanning the 5′ ends of the divergent *farE* and *farR* genes was amplified by PCR of *S. aureus* genomic DNA with primers *far*::*lux*-F and *farR*::*lux*-R, followed by digestion with BamHI and SalI, and ligation into pGY*lux* to create pGY*farR*::*lux*. The same primers were used in PCR with pLI*farR*1 as the template, and the amplified PCR product was cloned into pGY*lux* to create pGY*farR*1::*lux*, in which the −10 motif of P_{farR} harbors a G→A substitution. For the expression of recombinant 6×His-FarR and 6×His-^{H121Y}FarR, the FarR open reading frame was amplified by PCR from genomic DNA of *S. aureus* USA300 and *S. aureus* FAR7, respectively, using primers 6H*farR*-F and 6H*farR*-R. The PCR amplicons were digested with SacI and HindIII and ligated into SacI-HindIII-digested pQE30, creating pQE-FarR and pQE-^{H121Y}FarR.

Assays of bactericidal activity and reporter gene function. In preparation for bactericidal activity of antimicrobial fatty acids, overnight cultures were subcultured into 25 ml of TSB to prepare noninduced cells or in TSB containing 20 μM subinhibitory fatty acid to assay for inducible resistance. For complementation analyses, antibiotic was included in the overnight and initial subcultures but was omitted when cells were inoculated for assay of bactericidal activity. For the bactericidal assay, inoculum cultures were grown to mid-exponential phase (OD_{600}, 0.5) and then subcultured into triplicate or quadruplicate flasks of fresh TSB (OD_{600}, 0.01; approximately 2×10^6 CFU/ml) containing 100 μM linoleic acid. These cultures were then incubated with shaking at 37°C, and aliquots were withdrawn at hourly intervals for preparation of serial dilutions in sterile TSB. Aliquots of 10 μl were then spotted in quadruplicate onto TSB agar, and colonies were counted after 24 h of incubation. The mean from each quadruplicate

technical replicate was entered as a single data point for each flask, from which the mean and standard deviation from the biologic replicate flasks were determined.

For assay of reporter gene activity, *S. aureus* cultures harboring pGY*lux* and derivatives were subcultured into triplicate or quadruplicate flasks of TSB or TSB supplemented with fatty acids to achieve an initial OD_{600} of 0.01. The cultures were incubated at 37°C with orbital shaking, and samples were withdrawn at hourly intervals for OD_{600} determinations. Concurrently, four 200-μl aliquots of each sample were added to 96-well white opaque flat-bottom plates (Greiner Bio-one), and each well was supplemented with 20 μl of 0.1% (vol/vol) decanal in 40% ethanol. Luminescence measurements were immediately taken on a Synergy H4 hybrid reader (BioTek, Winooski, VT), with 1 s of integration and a gain of 200. Data values were recorded as relative light units (RLU), corrected for background by subtraction of values recorded from cultures harboring empty pGY*lux*. Data points were standardized for differences in growth by dividing RLU values by the recorded OD_{600} values of the cultures when samples were withdrawn.

Determination of MIC. Prior to determination of MIC to linoleic acid, inoculum cultures were grown to mid-exponential phase in 125-ml flasks containing 25 ml of TSB supplemented with antibiotics as appropriate for plasmid maintenance. Cultures containing pALC2073 vector and derivatives were additionally supplemented with 20 ng/ml anhydrotetracycline to stimulate expression of the P*xyl/tet* promoter. These cultures were then inoculated at OD_{600} of 0.01 into triplicate 20- by 150-mm glass culture tubes containing 3 ml of TSB supplemented with 0.1% DMSO and indicated concentrations of linoleic acid. Cultures were incubated at 37°C with vigorous shaking, and OD_{600} values were determined after 24h.

RNA isolation and 5′ rapid amplification of cDNA ends. RNA was isolated from *S. aureus* cells (USA300 or FAR7) grown to mid-exponential phase (OD_{600}, 0.5) in TSB supplemented with 20 μM linoleic acid. Cells equivalent to 3.0 OD_{600} units were harvested from triplicate cultures, and RNA extraction was performed using the E.Z.N.A. total RNA kit, with the addition of 0.25 μg/ml lysostaphin to the lysis solution. RNA integrity was visualized by agarose gel electrophoresis, and after quantification on a NanoDrop ND1000 UV-Vis spectrophotometer, cDNA synthesis was initiated using Superscript II reverse transcriptase (Invitrogen) and gene-specific primer *farR*-GSP1. The original mRNA template was subsequently removed by treatment with a mixture of RNase H (0.5 units) and RNase T1 (50 units) at 37°C for 30 min. The cDNA was then purified using the BioArray cDNA purification kit (Enzo Life Sciences), as per manufacturer's instructions, to eliminate unincorporated *farR*-GSP1 and dinucleoside triphosphates (dNTPs). A d(C) tail was added to the 3′ end of the purified cDNA using 20 units of terminal transferase (Roche) and 0.5 mM CTP. This was followed by two consecutive cycles of PCR using respective abridged anchor primer AAP and abridged universal amplification primer AUAP as forward primers and respective nested reverse primers *farR*-GSP2 and *farR*-GSP3. Following the second cycle of PCR, the amplification products were digested with SalI, using restriction sites incorporated into AUAP and *farR*-GSP3, and then ligated into pUC18 for transformation into *E. coli* DH5α. After plating on LB-ampicillin (LB-Amp) supplemented with 5-bromo-4-chloro-3-indolyl-β-D-galactopyranoside (X-Gal) and isopropyl thio-β-D-galactopyranoside (IPTG), white colonies were selected for sequencing using M13-F and M13-R primers that flank the multiple-cloning site of pUC18. The +1 transcription start site was identified as the first nucleotide following the poly(C) or poly(G) tail, depending on the orientation of the cloned insert.

Expression and purification of recombinant protein. Recombinant 6×His-FarR and 6×His-^{H121Y}FarR were expressed and purified from *E. coli* M15/pREP. Bacterial cultures were grown at 37°C in LB (Sigma-Aldrich) supplemented with 100 μg/ml ampicillin and 50 μg/ml kanamycin, to an OD_{600} of 0.8, before the addition of 0.1 mM IPTG and incubation at room temperature with shaking for an additional 18 h. Cells were harvested by centrifugation and resuspended in binding buffer (20 mM sodium phosphate, 0.5 M NaCl, 40 mM imidazole [pH 7.4]), lysed in a cell disruptor (Constant System Ltd.) at 25,000 lb/in^2, and then centrifuged for 50 min at 50,000 × *g* in a Beckman Coulter Optima L-900K ultracentrifuge, after which the soluble fraction was filtered through a 0.45-μm Acrodisc syringe filter (Pall Laboratory). The lysate was applied onto a 1-ml His-Trap nickel affinity column (GE Healthcare) equilibrated with binding buffer. After washing extensively with binding buffer, bound His-tagged protein was eluted over a linear imidazole gradient up to 0.5 M imidazole in 20 mM sodium phosphate buffer (pH 7.4). Column fractions were assessed by SDS-polyacrylamide gel electrophoresis to check for purity, and fractions containing FarR protein were pooled and dialyzed in 20 mM sodium phosphate and 0.5 M NaCl (pH 7.4) at 4°C. Protein concentration was determined by Bradford assay using Bio-Rad protein assay reagent.

Electrophoretic mobility shift assays. For EMSA, IRDye 800-labeled duplex and single-stranded nucleotide probes or PCR primers, as detailed in Table S1, were purchased from IDT. Complementary single-stranded oligonucleotides were mixed at 100 μM concentration in 10 mM Tris (pH 8.0) and 0.1 mM EDTA, heated at 95°C for 5 min, and then cooled at room temperature for 45 min to allow duplex formation. Each EMSA reaction was conducted in a 25-μl volume consisting of EMSA buffer (20% glycerol, 30 mM Tris-HCl [pH 8.0], 1 mM $MnCl_2$, 120 mM KCl, 1 mM $MgCl_2$, 16 mM dithiothreitol) supplemented with 5 pM of IRDye 800-labeled probe, up to 2 μM recombinant 6×His-FarR or 6×His-^{H121Y}FarR, 240 μg/ml bovine serum albumin (BSA), and 15.2 μg/ml poly[d(I-C)] in EMSA buffer. After incubation at room temperature for 60 min, individual samples were applied to a 6% polyacrylamide gel prepared in Tris-borate-EDTA buffer and electrophoresed in the same buffer system for 45 min at 120 V. The gels were then imaged using an Odyssey imager (Li-Cor Biosciences). In competition EMSA, unlabeled competitor probes harboring specific nucleotide substitutions were added in 50-fold excess relative to labeled probes.

Production of polyclonal antibodies and Western blotting. The production of FarR-specific polyclonal antibodies in New Zealand White rabbits was contracted to ProSci Incorporated (Poway, CA). Each of two animals was initially immunized with 200 μg of 6×His-FarR emulsified in complete Freund's adjuvant, followed by 100 μg of protein administered in incomplete Freund's adjuvant, at 2-week intervals for 6 weeks. The animals were then bled for collection of antiserum 2 weeks after the final immunization.

For preparation of cell lysates, *E. coli* DH5α harboring pLI*farR*, pLI*farER*, and derivatives were grown to mid-exponential phase in LB, and cells were harvested by centrifugation at 5,000 × *g* for 20 min, washed in ice cold 50 mM Tris-HCl, 5 mM EDTA, and 150 mM NaCl (pH 8.0), and then resuspended at 1/10 the original culture volume, in the same buffer supplemented with 1% (vol/vol) Triton X-100, 0.5% (vol/vol) SDS, and Pierce complete protease inhibitor cocktail. The cell suspensions were incubated for 2 h at room temperature on a rocking platform, followed by centrifugation at 5,000 × *g* for 20 min. The clarified cell lysate was then assayed for determination of total protein. For Western blots, samples containing 25 μg of total cell lysate protein were subjected to SDS-PAGE using a 12% polyacrylamide resolving gel. After transfer of proteins to FluoroTrans polyvinylidene difluoride (PVDF) membrane (Pall Life Sciences), the membranes were blocked by incubation in phosphate-buffered saline (PBS) supplemented with 5% nonfat skim milk powder and 10% horse serum (Sigma). Wash buffer and antibody dilution buffer consisted of PBS plus 0.05% Tween 20, and PBS-Tween supplemented with 2% skim milk powder. Primary anti-FarR antiserum was used at a dilution of 1:5,000, followed by secondary IRDye 800-conjugated goat anti-rabbit IgG (Jackson Immunoresearch Laboratories, Inc.). Membranes were imaged using an Odyssey imager (Li-Cor Biosciences).

Data analyses. Data points for growth, viability, reporter gene assays, and murine infection models were plotted and analyzed using GraphPad Prism version 7. Significant differences at specific time points were determined using GraphPad statistics functions.

SUPPLEMENTAL MATERIAL

Supplemental material for this article may be found at https://doi.org/10.1128/JB.00602-18.

SUPPLEMENTAL FILE 1, PDF file, 0.7 MB.

ACKNOWLEDGMENTS

We declare no potential conflicts of interest.

This work was supported by grants to M.J.M. and D.E.H. from the Natural Sciences and Engineering Research Council of Canada. J.E.T.S. and R.C.K. were recipients of Ontario Graduate Scholarship awards.

M.J.M. and D.E.H. contributed to the design of the study; H.A., R.C.K., K.A.F., and J.E.T.S. were responsible for data acquisition; H.A., D.E.H., and M.J.M. contributed to the analysis and interpretation of data; H.A. and M.J.M. shared in writing of the manuscript; and D.E.H. provided critical evaluation.

REFERENCES

1. Cuthbertson L, Nodwell JR. 2013. The TetR family of regulators. Microbiol Mol Biol Rev 77:440–475. https://doi.org/10.1128/MMBR.00018-13.
2. Kisker C, Hinrichs W, Tovar K, Hillen W, Saenger W. 1995. The complex formed between Tet repressor and tetracycline-Mg^{2+} reveals mechanism of antibiotic resistance. J Mol Biol 247:260–280. https://doi.org/10.1006/jmbi.1994.0138.
3. Alnaseri H, Arsic B, Schneider JET, Kaiser JC, Scinocca ZC, Heinrichs DE, McGavin MJ. 2015. Inducible expression of a resistance-nodulation-division-type efflux pump in *Staphylococcus aureus* provides resistance to linoleic and arachidonic acids. J Bacteriol 197:1893–1905. https://doi.org/10.1128/JB.02607-14.
4. Wertheim HF, Melles DC, Vos MC, van Leeuwen W, van Belkum A, Verbrugh HA, Nouwen JL. 2005. The role of nasal carriage in *Staphylococcus aureus* infections. Lancet Infect Dis 5:751–762. https://doi.org/10.1016/S1473-3099(05)70295-4.
5. Grkovic S, Brown MH, Schumacher MA, Brennan RG, Skurray RA. 2001. The staphylococcal QacR multidrug regulator binds a correctly spaced operator as a pair of dimers. J Bacteriol 183:7102–7109. https://doi.org/10.1128/JB.183.24.7102-7109.2001.
6. Jeng WY, Ko TP, Liu CI, Guo RT, Liu CL, Shr HL, Wang AHJ. 2008. Crystal structure of IcaR, a repressor of the TetR family implicated in biofilm formation in *staphylococcus epidermidis*. Nucleic Acids Res 36:1567–1577. https://doi.org/10.1093/nar/gkm1176.
7. Jefferson KK, Pier DB, Goldmann DA, Pier GB. 2004. The teicoplanin-associated locus regulator (TcaR) and the intercellular adhesin locus regulator (IcaR) are transcriptional inhibitors of the *ica* locus in *Staphylococcus aureus*. J Bacteriol 186:2449–2456. https://doi.org/10.1128/JB.186.8.2449-2456.2004.
8. Parsons JB, Yao J, Frank MW, Jackson P, Rock CO. 2012. Membrane disruption by antimicrobial fatty acids releases low-molecular-weight proteins from *Staphylococcus aureus*. J Bacteriol 194:5294–5304. https://doi.org/10.1128/JB.00743-12.
9. Bibel DJ, Miller SJ, Brown BE, Pandey BB, Elias PM, Shinefield HR, Aly R. 1989. Antimicrobial activity of stratum corneum lipids from normal and essential fatty acid-deficient mice. J Invest Dermatol 92:632–638. https://doi.org/10.1111/1523-1747.ep12712202.
10. Do TQ, Moshkani S, Castillo P, Anunta S, Pogosyan A, Cheung A, Marbois B, Faull KF, Ernst W, Chiang SM, Fujii G, Clarke CF, Foster K, Porter E. 2008. Lipids including cholesteryl linoleate and cholesteryl arachidonate contribute to the inherent antibacterial activity of human nasal fluid. J Immunol 181:4177–4187. https://doi.org/10.4049/jimmunol.181.6.4177.
11. Drake DR, Brogden KA, Dawson DV, Wertz PW. 2008. Thematic review series: skin lipids. Antimicrobial lipids at the skin surface. J Lipid Res 49:4–11. https://doi.org/10.1194/jlr.R700016-JLR200.
12. Shryock TR, Dye ES, Kapral FA. 1992. The accumulation of bactericidal lipids in staphylococcal abscesses. J Med Microbiol 36:332–336. https://doi.org/10.1099/00222615-36-5-332.
13. Fujihashi M, Nakatani T, Hirooka K, Matsuoka H, Fujita Y, Miki K. 2014. Structural characterization of a ligand-bound form of *Bacillus subtilis*

FadR involved in the regulation of fatty acid degradation. Proteins 82:1301–1310. https://doi.org/10.1002/prot.24496.
14. Yeo HK, Park YW, Lee JY. 2017. Structural basis of operator sites recognition and effector binding in the TetR family transcription regulator FadR. Nucleic Acids Res 45:4244–4254. https://doi.org/10.1093/nar/gkx009.
15. Parsons JB, Frank MW, Jackson P, Subramanian C, Rock CO. 2014. Incorporation of extracellular fatty acids by a fatty acid kinase-dependent pathway in *Staphylococcus aureus*. Mol Microbiol 92:234–245. https://doi.org/10.1111/mmi.12556.
16. Parsons JB, Broussard TC, Bose JL, Rosch JW, Jackson P, Subramanian C, Rock CO. 2014. Identification of a two-component fatty acid kinase responsible for host fatty acid incorporation by *Staphylococcus aureus*. Proc Natl Acad Sci U S A 111:10532–10537. https://doi.org/10.1073/pnas.1408797111.
17. Greenway DL, Dyke KG. 1979. Mechanism of the inhibitory action of linoleic acid on the growth of *Staphylococcus aureus*. J Gen Microbiol 115:233–245. https://doi.org/10.1099/00221287-115-1-233.
18. Fey PD, Endres JL, Yajjala VK, Widhelm TJ, Boissy RJ, Bose JL, Bayles KW. 2013. A genetic resource for rapid and comprehensive phenotype screening of nonessential *Staphylococcus aureus* genes. mBio 4:e00537-12. https://doi.org/10.1128/mBio.00537-12.
19. Corrigan RM, Foster TJ. 2009. An improved tetracycline-inducible expression vector for *Staphylococcus aureus*. Plasmid 61:126–129. https://doi.org/10.1016/j.plasmid.2008.10.001.
20. Ramos JL, Martinez-Bueno M, Molina-Henares AJ, Teran W, Watanabe K, Zhang X, Gallegos MT, Brennan R, Tobes R. 2005. The TetR family of transcriptional repressors. Microbiol Mol Biol Rev 69:326–356. https://doi.org/10.1128/MMBR.69.2.326-356.2005.
21. Pustell J, Kafatos FC. 1982. A high speed, high capacity homology matrix: zooming through SV40 and polyoma. Nucleic Acids Res 10:4765–4782. https://doi.org/10.1093/nar/10.15.4765.
22. Reese MG. 2001. Application of a time-delay neural network to promoter annotation in the *Drosophila melanogaster* genome. Comput Chem 26:51–56. https://doi.org/10.1016/S0097-8485(01)00099-7.
23. Yu Z, Reichheld SE, Savchenko A, Parkinson J, Davidson AR. 2010. A comprehensive analysis of structural and sequence conservation in the TetR family transcriptional regulators. J Mol Biol 400:847–864. https://doi.org/10.1016/j.jmb.2010.05.062.
24. Derouiche A, Bidnenko V, Grenha R, Pigonneau N, Ventroux M, Franz-Wachtel M, Nessler S, Noirot-Gros MF, Mijakovic I. 2013. Interaction of bacterial fatty-acid-displaced regulators with DNA is interrupted by tyrosine phosphorylation in the helix-turn-helix domain. Nucleic Acids Res 41:9371–9381. https://doi.org/10.1093/nar/gkt709.
25. Agari Y, Agari K, Sakamoto K, Kuramitsu S, Shinkai A. 2011. TetR-family transcriptional repressor *Thermus thermophilus* FadR controls fatty acid degradation. Microbiology 157:1589–1601. https://doi.org/10.1099/mic.0.048017-0.
26. Parsons JB, Frank MW, Subramanian C, Saenkham P, Rock CO. 2011. Metabolic basis for the differential susceptibility of Gram-positive pathogens to fatty acid synthesis inhibitors. Proc Natl Acad Sci U S A 108:15378–15383. https://doi.org/10.1073/pnas.1109208108.
27. Schumacher MA, Miller MC, Grkovic S, Brown MH, Skurray RA, Brennan RG. 2002. Structural basis for cooperative DNA binding by two dimers of the multidrug-binding protein QacR. EMBO J 21:1210–1218. https://doi.org/10.1093/emboj/21.5.1210.
28. Cue DR, Lei MG, Lee C. 2012. Genetic regulation of the intercellular adhesion locus in staphylococci. Front Cell Infect Microbiol 2:38. https://doi.org/10.3389/fcimb.2012.00038.
29. Agari Y, Sakamoto K, Kuramitsu S, Shinkai A. 2012. Transcriptional repression mediated by a TetR family protein, PfmR, from *Thermus thermophilus* HB8. J Bacteriol 194:4630–4641. https://doi.org/10.1128/JB.00668-12.
30. Liang J-L, Nie Y, Wang M, Xiong G, Wang Y-P, Maser E, Wu X-L. 2016. Regulation of alkane degradation pathway by a TetR family repressor *via* an autoregulation positive feedback mechanism in a Gram-positive Dietzia bacterium. Mol Microbiol 99:338–359. https://doi.org/10.1111/mmi.13232.
31. Christen S, Srinivas A, Bähler P, Zeller A, Pridmore D, Bieniossek C, Baumann U, Erni B. 2006. Regulation of the Dha operon of *Lactococcus lactis*: a deviation from the rule followed by the TetR family of transcription regulators. J Biol Chem 281:23129–23137. https://doi.org/10.1074/jbc.M603486200.
32. Bose JL, Daly SM, Hall PR, Bayles KW. 2014. Identification of the *Staphylococcus aureus vfrAB* operon, a novel virulence factor regulatory locus. Infect Immun 82:1813–1822. https://doi.org/10.1128/IAI.01655-13.
33. Krute CN, Rice KC, Bose JL. 2017. VfrB is a key activator of the Staphylococcus aureus SaeRS two-component system. J Bacteriol 199:e00828-16. https://doi.org/10.1128/JB.00828-16.
34. Ericson ME, Subramanian C, Frank MW, Rock CO. 2017. Role of fatty acid kinase in cellular lipid homeostasis and SaeRS-dependent virulence factor expression in *Staphylococcus aureus*. mBio 8:e00988-17. https://doi.org/10.1128/mBio.00988-17.
35. DeMars ZR, Bose JL. 2018. Redirection of metabolism in response to fatty acid kinase in *Staphylococcus aureus*. J Bacteriol 200:e00345-18. https://doi.org/10.1128/JB.00345-18.
36. Taylor DL, Ante VM, Bina XR, Howard MF, Bina JE. 2015. Substrate-dependent activation of the *Vibrio cholerae vexAB* RND efflux system requires *vexR*. PLoS One 10:e0117890. https://doi.org/10.1371/journal.pone.0117890.
37. Bina XR, Howard MF, Taylor-Mulneix DL, Ante VM, Kunkle DE, Bina JE. 2018. The *Vibrio cholera* RND efflux systems impact virulence factor production and adaptive responses via periplasmic sensor proteins. PLoS Pathog 14:e1006804. https://doi.org/10.1371/journal.ppat.1006804.
38. Ruiz C, Levy SB. 2014. Regulation of *acrAB* expression by cellular metabolites in *Escherichia coli*. J Antimicrob Chemother 69:390–399. https://doi.org/10.1093/jac/dkt352.
39. Buckner MMC, Blair JMA, La Ragione RM, Newcombe J, Dwyer DJ, Ivens A, Piddock LJV. 2016. Beyond antimicrobial resistance: evidence for a distinct role of the AcrD efflux pump in Salmonella biology. mBio 7:e01916-16. https://doi.org/10.1128/mBio.01916-16.
40. Grkovic S, Brown MH, Roberts NJ, Paulsen IT, Skurray RA. 1998. QacR is a repressor protein that regulates expression of the *Staphylococcus aureus* multidrug efflux pump QacA. J Biol Chem 273:18665–18673. https://doi.org/10.1074/jbc.273.29.18665.
41. Feng Y, Cronan JE. 2011. Complex binding of the FabR repressor of bacterial unsaturated fatty acid biosynthesis to its cognate promoters. Mol Microbiol 80:195–218. https://doi.org/10.1111/j.1365-2958.2011.07564.x.
42. Kloosterman TG, Van Der Kooi-Pol MM, Bijlsma JJ, Kuipers OP. 2007. The novel transcriptional regulator SczA mediates protection against Zn^{2+} stress by activation of the Zn^{2+}-resistance gene *czcD* in *Streptococcus pneumoniae*. Mol Microbiol 65:1049–1063. https://doi.org/10.1111/j.1365-2958.2007.05849.x.
43. van Kessel JC, Ulrich LE, Zhulin IB, Bassler L. 2013. Analysis of activator and repressor functions reveals the requirements for transcriptional control by LuxR, the master regulator of quorum sensing in *Vibrio harveyi*. mBio 4:e00378-13. https://doi.org/10.1128/mBio.00378-13.
44. Ball AS, Chaparian RR, van Kessel JC. 2017. Quorum sensing gene regulation by LuxR/HapR master regulators in Vibrios. J Bacteriol 199:e00105-17. https://doi.org/10.1128/JB.00105-17.
45. Novick RP. 1991. Genetic systems in staphylococci. Methods Enzymol 204:587–636. https://doi.org/10.1016/0076-6879(91)04029-N.
46. Cadieux B, Vijayakumaran V, Bernards MA, McGavin MJ, Heinrichs DE. 2014. Role of lipase from community-associated methicillin-resistant *Staphylococcus aureus* strain USA300 in hydrolyzing triglycerides into growth-inhibitory free fatty acids. J Bacteriol 196:4044–4056. https://doi.org/10.1128/JB.02044-14.
47. Nickerson N, Ip J, Passos DT, McGavin MJ. 2010. Comparison of Staphopain A (ScpA) and B (SspB) precursor activation mechanisms reveals unique secretion kinetics of proSspB (staphopain B), and a different interaction with its cognate staphostatin, SspC. Mol Microbiol 75:161–177. https://doi.org/10.1111/j.1365-2958.2009.06974.x.
48. Arsic B, Zhu Y, Heinrichs DE, McGavin MJ. 2012. Induction of the Staphylococcal proteolytic cascade by antimicrobial fatty acids in community acquired methicillin resistant *Staphylococcus aureus*. PLoS One 7:e45952. https://doi.org/10.1371/journal.pone.0045952.
49. Diep BA, Gill SR, Chang RF, Phan TH, Chen JH, Davidson MG, Lin F, Lin J, Carleton HA, Mongodin EF, Sensabaugh GF, Perdreau-Remington F. 2006. Complete genome sequence of USA300, an epidemic clone of community-acquired meticillin-resistant *Staphylococcus aureus*. Lancet 367:731–739. https://doi.org/10.1016/S0140-6736(06)68231-7.
50. Bae T, Schneewind O. 2006. Allelic replacement in *Staphylococcus aureus* with inducible counter-selection. Plasmid 55:58–63. https://doi.org/10.1016/j.plasmid.2005.05.005.
51. Li M, Rigby K, Lai Y, Nair V, Peschel A, Schittek B, Otto M. 2009. *Staphylococcus aureus* mutant screen reveals interaction of the human antimicrobial peptide dermcidin with membrane phospholipids. Antimi-

crob Agents Chemother 53:4200–4210. https://doi.org/10.1128/AAC.00428-09.
52. Lee CY, Iandolo JJ. 1986. Lysogenic conversion of staphylococcal lipase is caused by insertion of the bacteriophage L54a genome into the lipase structural gene. J Bacteriol 166:385–391. https://doi.org/10.1128/jb.166.2.385-391.1986.
53. Bateman BT, Donegan NP, Jarry TM, Palma M, Cheung AL. 2001. Evaluation of a tetracycline-inducible promoter in *Staphylococcus aureus in vitro* and i*n vivo* and its application in demonstrating the role of *sigB* in microcolony formation. Infect Immun 69:7851–7857. https://doi.org/10.1128/IAI.69.12.7851-7857.2001.
54. Mesak LR, Yim G, Davies J. 2009. Improved *lux* reporters for use in *Staphylococcus aureus*. Plasmid 61:182–187. https://doi.org/10.1016/j.plasmid.2009.01.003.